The Plant Journal (2007) doi: 10.1111/j.1365-313X.2007.03198.x

A mitochondrial protein homologous to the mammalian peripheral-type benzodiazepine receptor is essential for stress adaptation in plants

Wolfgang Frank[1,*], Kim-Miriam Baar[1,†], Enas Qudeimat[1], Mayada Woriedh[1], Ali Alawady[2], Diah Ratnadewi[1,‡], Louis Gremillon[1], Bernhard Grimm[2] and Ralf Reski[1]

[1]*Plant Biotechnology, Faculty of Biology, University of Freiburg, Schaenzlestr. 1, 79104 Freiburg, Germany, and*
[2]*Institute of Biology, Plant Physiology, Humboldt University Berlin, Philippstraße 13, 10115 Berlin, Germany*

Received 19 December 2006; revised 26 April 2007; accepted 15 May 2007.
*For correspondence (fax +49 (0) 761 203 6945; e-mail wolfgang.frank@biologie.uni-freiburg.de).
†Present address: Department of Cardiology, Faculty of Medicine, University of Freiburg, Breisacher Str. 33, 79106 Freiburg.
‡Present address: Department of Biology, Bogor Agricultural University, Jl. Raya Pajajaran, Bogor, Indonesia.

Summary

The cloning of abiotic stress-inducible genes from the moss *Physcomitrella patens* led to the identification of the gene *PpTSPO1*, encoding a protein homologous to the mammalian mitochondrial peripheral-type benzodiazepine receptor and the bacterial tryptophane-rich sensory protein. This class of proteins is involved in the transport of intermediates of the tetrapyrrole biosynthesis pathway. Like the mammalian homologue, the PpTSPO1 protein is localized to mitochondria. The generation of *PpTSPO1*-targeted moss knock-out lines revealed an essential function of the gene in abiotic stress adaptation. Under stress conditions, the *PpTSPO1* null mutants show elevated H_2O_2 levels, enhanced lipid peroxidation and cell death, indicating an important role of PpTSPO1 in redox homeostasis. We hypothesize that PpTSPO1 acts to direct porphyrin precursors to the mitochondria for heme formation, and is involved in the removal of photoreactive tetrapyrrole intermediates.

Keywords: *Physcomitrella patens*, abiotic stress tolerance, mitochondria, tetrapyrroles, reactive oxygen species.

Introduction

In animals, tetrapyrrole biosynthesis starts in the mitochondria, continues in the cytoplasm up to the formation of coproporphyrinogen III, and finishes in the mitochondria with the synthesis of protoheme. In contrast, the subcellular localization of the tetrapyrrole biosynthesis pathway in plants is distributed to plastids and mitochondria. All tetrapyrrole end products are synthesized in plastids, with the exception that the last two steps of heme synthesis are additionally found in mitochondria (Cornah *et al.*, 2003; Papenbrock and Grimm, 2001). The most abundant tetrapyrrole end product in plants is chlorophyll. Heme serves as a co-factor for proteins in diverse cellular processes such as respiration (cytochromes) and oxygen metabolism (catalases, peroxidases and NADPH oxidases) (Beale and Weinstein, 1990; Grimm, 1998). The plant tetrapyrrole metabolic pathway is also needed for the synthesis of siroheme, which is a co-factor for the nitrite and sulphite reductases required for the assimilation of inorganic nitrogen and sulphur. Finally, the linear tetrapyrrole phytochromobilin is derived from protoheme and is assembled with phytochrome.

Although chlorophyll is confined to the chloroplast, as is siroheme, heme is present in all cellular compartments, and phytochrome operates in the cytosol and in the nucleus (Kircher *et al.*, 2002; Moulin and Smith, 2005). The subcellular partition of the plant tetrapyrrole pathway, leading to the targeting of diverse end products into different subcellular compartments, necessitates a coordinated distribution of tetrapyrrole intermediates between the two organelles, plastids and mitochondria. Moreover, the pool of tetrapyrrole intermediates and end products has to be tightly controlled, as they can be excited by light and their photoreactivity can generate radicals and singlet oxygen species. The tetrapyrrole biosynthesis pathway is substantially regulated by environmental stimuli, and during plant development at different levels of gene expression for

certain enzymes of this pathway (Grimm, 1998; Reinbothe and Reinbothe, 1996).

Recently, the mammalian adenosine 5′-triphosphate-binding cassette transporter ABCB6, which is located at the outer mitochondrial membrane, was found to be required for mitochondrial porphyrin uptake and heme biosynthesis (Krishnamurthy *et al.*, 2006). A previously reported key element in the regulation of steroid biosynthesis in mammals is the 18-kDa peripheral-type benzodiazepine receptor, which mediates mitochondrial cholesterol import (Li and Papadopoulos, 1998; Papadopoulos, 1998). Recently, a new nomenclature for this protein family was suggested based on the protein structure and molecular function (Papadopoulos *et al.*, 2006) designating these proteins translocator proteins (TSPO). The mammalian TSPO is localized in the outer mitochondrial membrane (Papadopoulos *et al.*, 1994) where it is closely associated with other proteins, such as the 34-kDa voltage-dependent anion channel and the inner membrane adenine nucleotide carrier (McEnery *et al.*, 1992). Moreover, TSPO was shown to possess the highest binding affinity for protoporphyrin IX, indicating an involvement in the tetrapyrrole metabolism in mouse erythroleukemia cells (Taketani *et al.*, 1994). It was suggested that TSPO is involved in porphyrin transport, and is a critical factor in erythroid-specific induction of heme biosynthesis genes. More than ten years ago Yeliseev and Kaplan (1995) reported on the tryptophane-rich sensory protein (TspO) from the α-proteobacterium *Rhodobacter sphaeroides*, with significant similarities to the mammalian TSPO. TspO is involved in the negative regulation of photosynthesis genes in response to oxygen. Nevertheless, evidence that TspO directly regulates the expression of photosynthesis genes in *R. sphaeroides* was not provided. The TspO protein is localized at the outer membrane of *R. sphaeroides* cells (Yeliseev and Kaplan, 1995) and functions in the export of excessive intermediates of the tetrapyrrole pathway (Yeliseev and Kaplan, 1999). Furthermore, the rat TSPO homologue was able to substitute for TspO, indicated by the suppression of photosynthesis genes in response to oxygen (Yeliseev *et al.*, 1997). This suggests an evolutionary and functional relationship between the bacterial TspO and TSPO. Additionally, Lindemann *et al.* (2004) provided evidence that a homologous protein to the mammalian TSPO and the *R. sphaeroides* TspO is also present in *Arabidopsis thaliana* and other plants. Transport studies with the recombinant Arabidopsis TSPO in *Escherichia coli* revealed a benzodiazepine-stimulated high-affinity uptake of protoporphyrin and cholesterol, leading to the hypothesis that the Arabidopsis homologue functions in the transport of protoporphyrinogen IX to the mitochondrial site of protoheme formation. Immunogold staining using an antimouse TSPO peptide antibody led to signals both at the outer thylakoid membrane of plastids and in the mitochondria of *Digitalis lanata* leaves. An antibody raised against the Arabidopsis TSPO homologue recognized proteins with a molecular mass of 19–20 kDa in mitochondria of Arabidopsis, potato and *D. lanata*. Even though substrate binding properties of the Arabidopsis TSPO were initially determined, its role in transport and regulation of plant metabolism is still unknown.

Here, we report on the isolation of an abiotic stress-induced TSPO homologue from the moss *Physcomitrella patens*. Functional studies with generated targeted moss knock-out lines suggest an essential role of the protein in plant stress adaptation.

Results

Isolation of PpTSPO1 *from* P. patens

Comparison of mRNA pools of the untreated and dehydrated moss *P. patens* by differential display reverse transcription-polymerase chain reaction (DDRT-PCR) facilitated the identification of genes induced upon dehydration. One arbitrary primer (see Experimental procedures) gave rise to a cDNA fragment derived from the cDNA pool of dehydrated tissue, which was absent in the RT-PCR reaction using the cDNA from untreated plants. The PCR fragment was cloned, sequenced and used for the identification of a 1041-bp full-length cDNA sequence, containing an open reading frame coding for a protein of 198 amino acids, with a predicted molecular mass of 21.8 kDa. BLAST searches with the predicted amino acid sequence revealed homology to proteins from bacteria, animals and plants, including TspO from *R. sphaeroides*, (Yeliseev and Kaplan, 1995), the human mitochondrial TSPO (Papadopoulos, 1998) and the TSPO-like transporter from Arabidopsis (Lindemann *et al.*, 2004) (Table S1). Based on the similarity with the well-characterized TspO protein from *R. sphaeroides*, the isolated gene from *P. patens* was designated *PpTSPO1* (*P. patens* tryptophane-rich sensory protein 1). An alignment of homologous proteins from different kingdoms performed with the CLUSTALW multiple sequence alignment program (Thompson *et al.*, 1994) is shown in Figure S1. BLAST searches performed in the Genbank expressed sequence tag (EST) database revealed that PpTSPO1 shares the highest similarity to a deduced protein sequence from the desiccation-tolerant moss *Tortula ruralis*. Protein topology prediction for PpTSPO1 using the TMHMM 2.0 analysis software (Krogh *et al.*, 2001) suggests the presence of five transmembrane helices (Figure S2). A multiple sequence alignment of the thirty closest homologues from bacteria, plants and animals found so far using the topology prediction algorithm TMAP (Persson and Argos, 1994, 1996) revealed three conserved transmembrane-spanning regions (positions 67–91, 148–168 and 186–214 amino acids of the alignment; Figure S2) in all protein sequences, indicating

that these proteins exert their function as integral membrane proteins.

PpTSPO1 *is induced by abiotic stresses and abscisic acid (ABA)*

To verify the induction of *PpTSPO1* by drought stress, RNA blot analysis was performed with RNA from dehydrated *P. patens* plants. As many dehydration-responsive genes are also induced by other abiotic stresses, we investigated the *PpTSPO1* expression pattern in response to cold and salt. We have previously shown that the induction of stress-responsive genes in *P. patens* is mediated by the phytohormone ABA, which complies with the role of ABA as a second messenger in stress-induced gene expression in vascular plants (Frank *et al.*, 2005b). Thus, *PpTSPO1* expression was also examined for its ABA-dependent control. After 1 h of the various stress treatments and application of ABA the *PpTSPO1* mRNA levels increased rapidly and strongly, whereas only weak quantities of *PpTSPO1* mRNA could be detected in untreated control plants (Figure 1). Thus, *PpTSPO1* expression is induced by different ABA-dependent abiotic stress-related pathways. *PpTSPO1* expression analyses 15 and 30 min after the application of different stimuli revealed a rapid induction of the gene in response to ABA, whereas the expression in response to NaCl and dehydration was not markedly altered (Figure 1). Until now, a stress-induced expression of this class of genes in plants was not reported. Based on the specific expression pattern of *PpTSPO1* in response to abiotic stress, we suggest a functional role of the encoded protein in abiotic stress adaptation in *P. patens*.

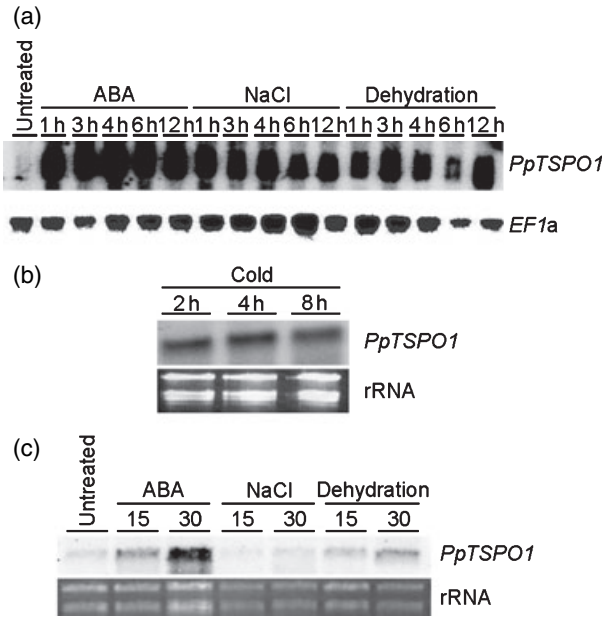

Figure 1. Expression analysis of *PpTSPO1* in response to abiotic stress and abscisic acid (ABA).
(a) *Physcomitrella patens* plants were dehydrated, treated with 20 μM ABA or treated with 250 mM NaCl for the indicated time periods. Untreated plants served as controls. A 10-μg sample of each RNA was loaded for RNA gel blot. The RNA blot was hybridized with a *PpTSPO1* cDNA probe and an *EF1α* control sample to verify equal loading of the gel.
(b) *P. patens* plants were kept on ice for the indicated time periods. A 10-μg sample of each RNA was loaded for RNA gel blot. The blot was hybridized with a *PpTSPO1* cDNA fragment. The lower panel shows ethidium bromide stained rRNA bands to indicate equal loading of the samples.
(c) *P. patens* plants were dehydrated, treated with 20 μM ABA or treated with 250 mM NaCl for 15 and 30 min, respectively. Untreated plants served as controls. A 10-μg sample of each RNA was loaded for RNA gel blot and hybridized with a *PpTSPO1* cDNA probe. The lower panel shows ethidium bromide stained rRNA bands to indicate equal loading of the samples.

PpTSPO1 is localized to mitochondria

The topology prediction for PpTSPO1 indicated the presence of five membrane-spanning regions, suggesting that PpTSPO1 represents an integral membrane protein. Attempts to predict the subcellular localization of PpTSPO1 by making use of common target prediction tools did not lead to conclusive results. For a genuine proof of subcellular localization of PpTSPO1, we have generated a *PpTSPO1::GFP* fusion construct containing the open reading frame of *PpTSPO1* and the green fluorescent protein (GFP) under the control of the CaMV *35S* promoter. The resulting construct was used for transfection of *P. patens* protoplasts, which were analysed by confocal laser scanning microscopy 48 h after the transfection (Figure 2). GFP fluorescence was detected in mitochondria of transformed protoplasts and the observed GFP pattern was identical to already described mitochondria-localized proteins in *P. patens*, like the

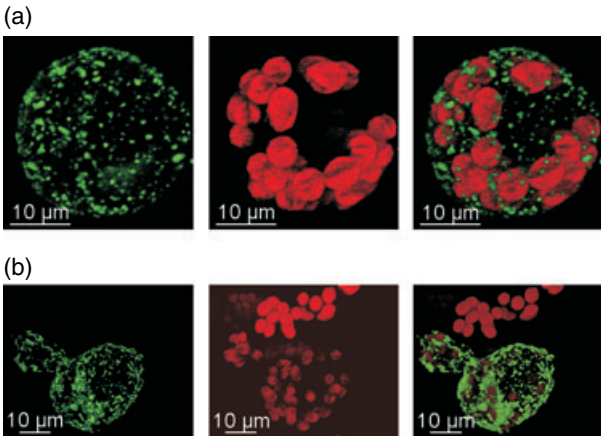

Figure 2. Subcellular localization of PpTSPO1. *Physcomitrella patens* protoplasts were transfected with a *PpTSPO1::GFP* C-terminal fusion construct. At 48 h after transfection protoplasts were analysed by confocal laser scanning microscopy.
(a) and (b) Two independent protoplasts transfected with the *PpTSPO1::GFP* construct. Left panels, green fluorescent protein (GFP) fluorescence; middle panels, chlorophyll autofluorescence; right panels, overlay of red chlorophyll and green GFP fluorescence.

phage-type RNA polymerases PpRpoT1 and PpRpoT2 (Richter *et al.*, 2002).

Generation of targeted PpTSPO1 *knock-out mutants*

Based on its unique ability to integrate DNA into its nuclear genome by means of homologous recombination (Schaefer, 2001), *P. patens* has become a versatile plant model system for reverse genetics approaches (Strepp *et al.*, 1998). For the functional analysis of *PpTSPO1* we prepared a *PpTSPO1* gene disruption construct by inserting an *npt*II selection marker cassette into the *PpTSPO1* cDNA (Figure 3a). After the transfection of *P. patens* protoplasts with the gene disruption construct and subsequent selection, plants were screened for the disruption of the *PpTSPO1* genomic locus. PCR was performed on genomic DNA of transgenic lines and wild-type plants with primers spanning the insertion site of the *npt*II selection marker cassette (Figure 3b). Genomic DNA of those transgenic lines, which generates a PCR product identical to the one obtained from wild-type plants, was considered to be subjected to an illegitimate integration of the knock-out construct. Alternatively, transgenic lines containing genomic DNA that could not be amplified, or generated a 1.5-kb bigger PCR product according to the size of the *npt*II cassette, were considered to be putative *PpTSPO1* knock-out lines. A total of 82 transgenic lines were screened, and 20 lines (24.3%) failed to give rise to a PCR product. To validate the generation of loss-of-function mutants, six of these lines were chosen to analyse the *PpTSPO1* transcript by RT-PCR and RNA gel blot analysis (Figure 3c,d). For RT-PCR studies primers were used that spanned the integrated *npt*II cassette. As the *PpTSPO1* gene was found to be induced by abiotic stress and ABA, wild-type control plants and the transgenic lines were treated with 20 μM ABA for 2 h. PCR reactions using cDNA derived from the six knock-out lines failed to give rise to an amplification product, whereas the control PCR with cDNA derived from wild-type plants produced an amplicon of the expected size. Additionally, the *PpTSPO1* transcript was not detected by RNA gel blot analysis using RNA from ABA-treated knock-out lines, confirming that the integration of the *PpTSPO1* disruption construct led to *PpTSPO1* null mutants.

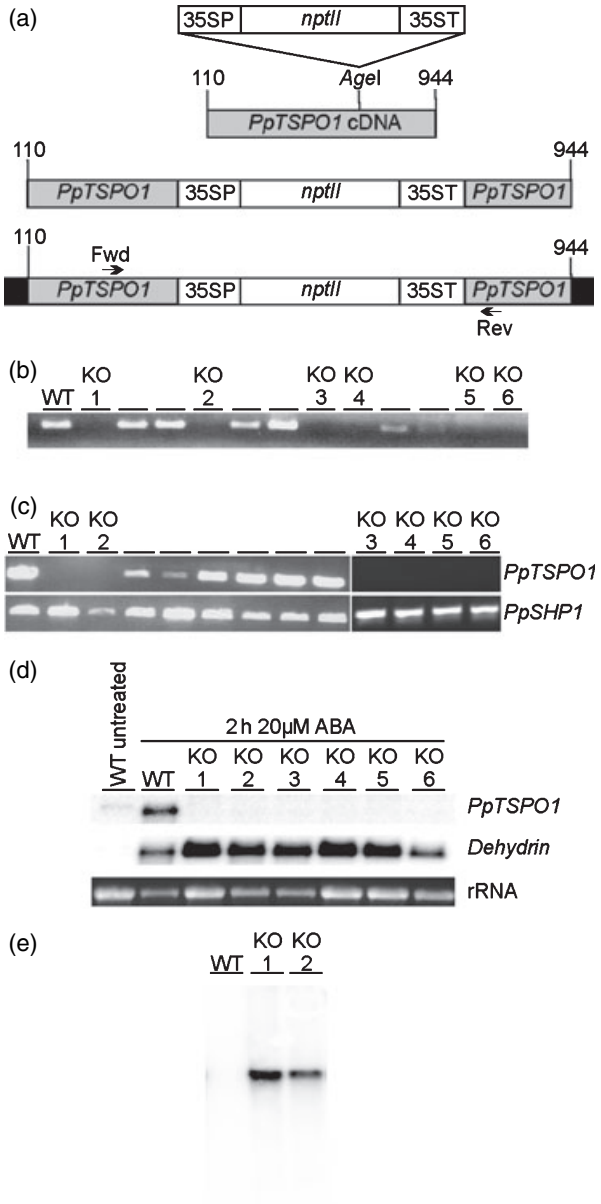

Figure 3. Generation and molecular analysis of *PpTSPO1* knock-out lines.
(a) Scheme illustrating the generation of the *PpTSPO1* knock-out construct. The middle panel illustrates the resulting *PpTSPO1* knock-out construct. The lower panel depicts the genomic structure of the *PpTSPO1* locus after integration of the *PpTSPO1* knock-out construct by homologous recombination. The primers that were used for molecular analyses of the transgenic lines are indicated by arrows. White box, *npt*II cassette; grey boxes, *PpTSPO1* cDNA fragments; black boxes, genomic *PpTSPO1* locus.
(b) Molecular analysis using genomic DNA to identify *PpTSPO1* knock-out lines. One representative gel showing polymerase chain reaction (PCR) reactions performed with primers Fwd and Rev (c.f. a). Six transgenic lines that failed to give rise to PCR products are indicated (KO 1–6); WT, wild-type control.
(c) Analysis of the *PpTSPO1* transcript in wild type and *PpTSPO1* knock-out lines by RT-PCR. PCR reactions were performed using cDNA prepared from abscisic acid (ABA)-treated plants. Upper panel: RT-PCR using the primers Fwd and Rev. Verified null-mutants are indicated by KO 1–6. Lower panel: control PCR using primers derived from the ABA-induced gene *PpSHP1* to indicate integrity of the cDNA.
(d) RNA gel blot analysis of wild-type (WT) and *PpTSPO1* knock-out lines (KO 1–6). RNA gel blot using 5 μg of total RNA hybridized with *PpTSPO1* and a hybridization probe derived from an ABA-induced dehydrin gene to monitor effective ABA treatment. Lower panel: ethidium bromide stained rRNA to indicate loading of the gel.
(e) Genomic Southern blot of wild-type (WT) and two *PpTSPO1* knock-out lines 1 and 2 (KO 1 and 2). A DNA blot with 10 μg genomic DNA digested with *Sac*I, which does not cut within the *npt*II cassette, was hybridized with the complete *npt*II selection marker cassette. Both knock-out lines show a single hybridizing band, indicating a single insertion event of the *PpTSPO1* knock-out construct in both lines.

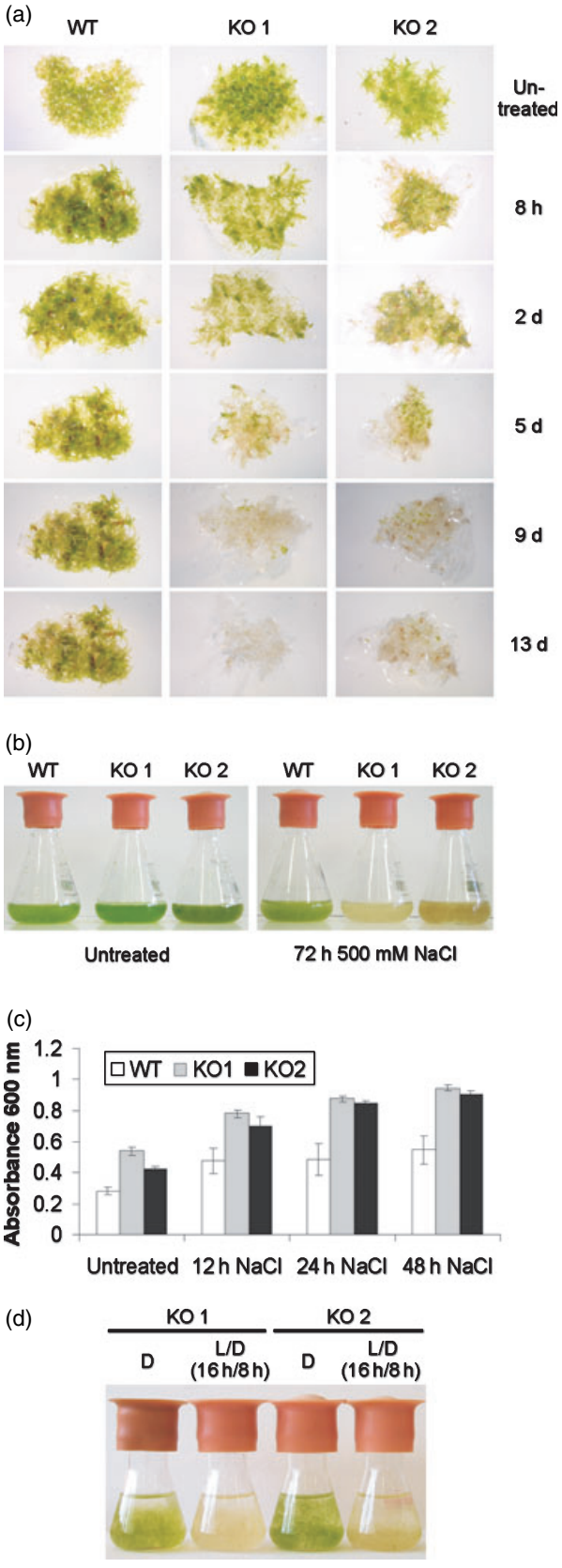

Independently, the six knock-out lines were analysed by flow cytometry to exclude the generation of diploid lines by protoplast fusion during the transformation process. All six knock-out lines were shown to be haploid (data not shown). To exclude additional integration sites of the *PpTSPO1* knock-out construct within the nuclear DNA, two of the knock-out lines were subjected to genomic Southern blot analysis (Figure 3e). A DNA fragment comprising the complete *npt*II selection marker cassette present in the knock-out construct was used as a hybridization probe. The resulting hybridization pattern demonstrates a single integration event in both mutant lines. These two lines were used for further experimental studies.

PpTSPO1 is essential for salt stress adaptation

Under standard growth conditions the *PpTSPO1* knock-out lines did not show any phenotypic differences compared with *P. patens* wild-type plants (Figure 4a), suggesting that under favourable growth conditions the encoded protein does not contribute to phenotypic distinction. However, the stress-induced expression of *PpTSPO1* suggests a role of this protein during the abiotic stress response in *P. patens*. The tolerance of *P. patens* plants to various abiotic stress conditions was determined previously (Frank *et al.*, 2005b), where we could demonstrate that *P. patens* plants are able to tolerate elevated NaCl concentrations. To obtain functional data on the role of *PpTSPO1* during the stress adaptation, we compared the two *PpTSPO1* knock-out lines with wild-type plants for their ability to withstand enhanced NaCl concentrations. Wild-type plants and both knock-out lines were grown on standard medium supplemented with 400, 500 and 600 mM NaCl, respectively. After only 8 h of growth on salt medium, the two *PpTSPO1* knock-out lines showed phenotypic deviations compared with wild-type plants, like shrinking of gametophores and protonema filaments, and bleaching of the green tissue. The most prominent differences between the knock-out lines and wild-type plants during further growth on the NaCl plates were observed at

Figure 4. NaCl treatment of *Physcomitrella patens* wild-type plants and *PpTSPO1* knock-out lines.
(a) *P. patens* wild-type plants (WT) and plants of the *PpTSPO1* knock-out lines (KO 1, KO 2) were grown on standard growth medium supplemented with 600 mM NaCl. From each line, 10 plants were analysed in two independent experiments. Pictures from representative plants were taken after the indicated time periods.
(b) *P. patens* wild-type (WT) and *PpTSPO1* knock-out lines (KO 1, KO 2) were grown in standard liquid medium (untreated) and liquid medium supplemented with 500 mM NaCl and photographed after 72 h post-inoculation.
(c) Cell death was measured spectrophotometrically by Evans blue staining in wild-type plants and *PpTSPO1* knock-out lines. Plants were grown in standard growth medium (untreated) or in medium supplemented with 500 mM NaCl for the indicated time periods. Error bars indicate SD ($n = 3$).
(d) Growth of *PpTSPO1* knock-out lines in the dark (D) and under standard growth conditions (L/D 16 h/8 h) for 72 h in the presence of 500 mM NaCl.

the 600 mM NaCl concentration (Figure 4a). Thirteen days after transfer onto 600 mM NaCl all plants from the two knock-out lines were almost completely bleached, whereas the wild-type plants tolerated the elevated NaCl concentration without phenotypic changes. We observed similar responses of wild-type and *PpTSPO1* knock-out lines in liquid medium supplemented with 500 mM NaCl. Only 3 days after inoculation of the plants in the NaCl-containing medium, the two mutant lines were completely bleached, whereas the wild-type plants did not show macroscopic differences (Figure 4b). The observed bleaching of the *PpTSPO1* knock-out lines in response to elevated NaCl concentrations suggests enhanced photooxidative damage of photosynthetic pigments, which are often accompanied by irreversible deleterious effects leading to cell death. As an indication for loss of membrane integrity and resulting cell death, cultures were stained with Evans blue. Cell death was measured from wild-type plants and the two *PpTSPO1* knock-out lines grown in liquid standard medium or medium supplemented with 500 mM NaCl (Figure 4c). Interestingly, the two knock-out lines already showed enhanced Evans blue staining under normal growth conditions, which could be indicative for the need of *PpTSPO1* expression under normal culture conditions. The values determined at 500 mM NaCl indicate that high NaCl concentrations severely affect the *PpTSPO1* knock-out lines, thus confirming the results obtained from the growth experiment on NaCl-containing medium. To study the influence of light, which might cause photooxidative damage, the two *PpTSPO1* knock-out lines were grown in liquid medium in the presence of 500 mM NaCl either in constant darkness or under normal light conditions. After 3 days the plants that were grown under normal light conditions were completely bleached, whereas the plants grown in darkness were unaffected and remained green (Figure 4d). The decreased tolerance of the two *PpTSPO1* knock-out lines reveals that PpTSPO1 is an essential protein required for salt stress adaptation in *P. patens.* The light-dependent susceptibility to enhanced concentrations of NaCl observed for the *PpTSPO1* knock-out lines suggests an involvement of the PpTSPO1 protein in the control of photooxidative damage.

PpTSPO1 *knock-out lines produce elevated levels of hydrogen peroxide*

The elevated chlorophyll bleaching in the *PpTSPO1* knock-out lines compared with wild-type plants observed during growth on medium containing NaCl suggested an enhanced generation of reactive oxygen species (ROS) in the mutant lines. Quantitative H_2O_2 measurements and detection of H_2O_2 by staining with 3, 3′-diaminobenzidine (DAB) were performed with wild-type plants and *PpTSPO1* knock-out lines after exposure to 500 mM NaCl. The H_2O_2

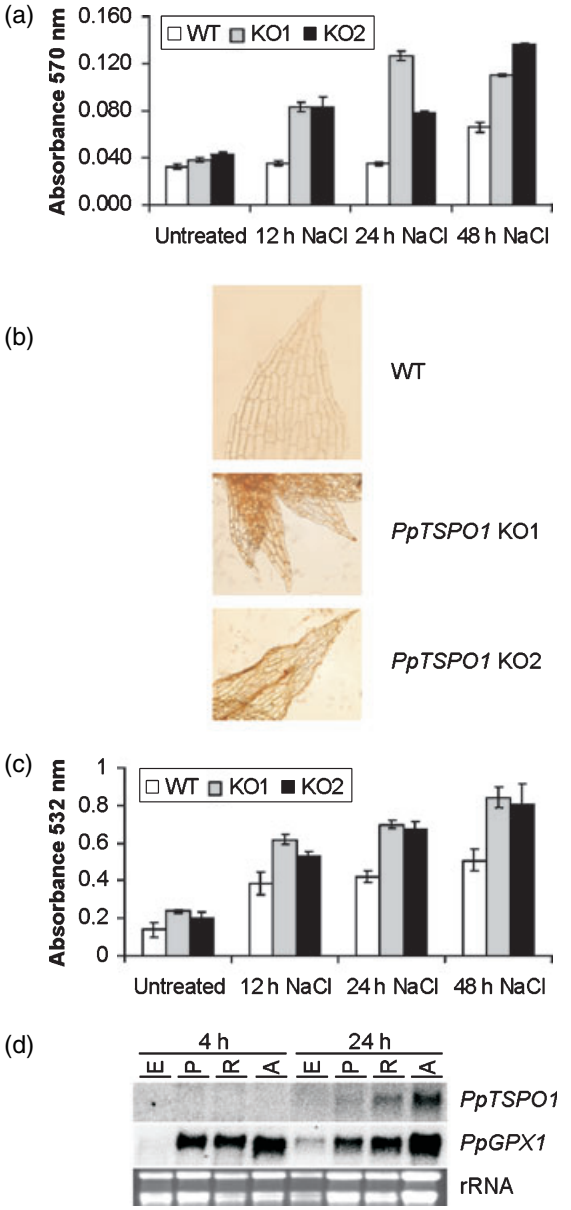

Figure 5. H_2O_2 detection, measurement of lipid peroxidation and analysis of *PpTSPO1* expression in response to oxidative stress.
(a) *Physcomitrella patens* wild-type plants (WT) and *PpTSPO1* knock-out lines (KO 1, KO 2) were grown in standard liquid medium (untreated) and liquid medium supplemented with 500 mM NaCl. H_2O_2 was measured at the indicated times. Absorbance values indicate absorption of the produced oxidation product resofurin at 570 nm. Error bars indicate SD ($n = 3$).
(b) H_2O_2 levels were visualized with 3, 3′-diamonobenzidine in wild-type plants (WT) and *PpTSPO1* mutants grown in the presence of 500 mM NaCl for 24 h.
(c) Wild-type plants and *PpTSPO1* mutants were grown in the presence of 500 mM NaCl and lipid peroxidation was determined at the indicated time points by measuring malone dialdehyde levels, as described in Experimental procedures. Error bars indicate SD ($n = 3$).
(d) RNA gel blot analysis using 10 μg of RNA isolated from wild-type plants treated with 0.5 μM paraquat (P), 4 μM rotenone (R), 1 μM antimycin A (A) and 0.1% ethanol (E; control). Upper panel: blot hybridized with *PpTSPO1* cDNA probe. Middle panel: blot hybridized with a *PpGPX1* cDNA probe. Lower panel: ethidium bromide stained rRNA to indicate equal loading.

levels were elevated in both *PpTSPO1* knock-out lines compared with wild-type plants after 12, 24 and 48 h of the NaCl treatment (Figure 5a). These measurements were further confirmed by the DAB staining of *PpTSPO1* mutants as well as wild-type plants 24 h after exposure to 500 mM NaCl (Figure 5b). ROS are harmful compounds that cause a number of adverse modifications within the cell, like protein oxidation, DNA damage and lipid peroxidation (Mittler, 2002). To analyse the effect of the elevated ROS levels detected in the *PpTSPO1* knock-out lines, lipid peroxidation after exposure to 500 mM NaCl was determined (Figure 5c). The two *PpTSPO1* knock-out lines showed enhanced levels of lipid peroxidation, even under standard growth conditions. Upon NaCl stress the degree of lipid peroxidation increased in both the wild-type and *PpTSPO1* knock-out lines. However, the degree of lipid peroxidation measured in both *PpTSPO1* knock-out lines was above the levels detected in wild-type plants. These findings are in agreement with the observed elevated levels of H_2O_2 in the *PpTSPO1* mutants, and imply a role of PpTSPO1 in the prevention of ROS formation or scavenging of ROS. As ROS could act as a direct stimulus to induce *PpTSPO1* expression, we asked if the site of ROS production may influence *PpTSPO1* gene expression. Wild-type plants were treated with paraquat (methylviologen), an inhibitor of photosynthetic electron transport (Dodge, 1971), and the two mitochondrial electron transport inhibitors rotenone and antimycin A (Ohnishi *et al.*, 1966). These inhibitors impair the electron transport in the photosynthetic and respiratory electron chains, respectively. In consequence, ROS will be generated by the transfer of electrons to oxygen. To monitor the generation of ROS by the different inhibitors, a *P. patens* gene homologous to plant glutathione peroxidases (*PpGPX1*; accession number DQ645821), which are known to be upregulated by elevated ROS levels, was used. The mRNA levels of the *PpGPX1* control were upregulated 4 h after application of the three inhibitors, indicating elevated ROS levels caused by the inhibitor treatments (Figure 5d). At this time point increased *PpTSPO1* mRNA levels were not observed. The same results were obtained after 8 and 12 h of inhibitor treatments (data not shown). However, after 24 h the *PpTSPO1* mRNA levels increased in plants treated with the mitochondrial inhibitors rotenone and antimycin A, but not in response to the photosynthetic inhibitor paraquat. In contrast to the rapid accumulation of *PpTSPO1* mRNA by abiotic stress and ABA, the induction of *PpTSPO1* by oxidative stress seems to be less effective when compared with other oxidative stress-responsive genes like *PpGPX1*. However, the *PpTSPO1* expression is dependent on the site of ROS generation. In agreement with the subcellular localization of the PpTSPO1 protein, elevated *PpTSPO1* mRNA levels were caused only by mitochondrial respiratory electron chain inhibitors. This finding suggests a specific role for PpTSPO1 in the control of ROS in mitochondria.

PpTSPO1 *knock-out lines show elevated heme and protoporphyrin IX levels in response to abiotic stress*

The Arabidopsis TSPO-like protein is able to transport protoporphyrin IX (Lindemann *et al.*, 2004). We hypothesized that the loss of PpTSPO1 will result in a decreased protoporphyrinogen transport into the mitochondria, and in turn would lead to decreased mitochondrial heme levels. As *PpTSPO1* mRNA levels are markedly increased upon dehydration, wild-type plants and the two *PpTSPO1* knock-out lines were subjected to dehydration and subsequently heme concentrations were analysed (Figure 6a). The heme levels in wild-type plants as well as in *PpTSPO1* knock-out lines increased in response to dehydration, which may reflect an enhanced demand for heme as prosthetic group upon stress conditions. Intriguingly, the two *PpTSPO1* knock-out lines showed higher heme levels compared with the wild-type plants, which could result from elevated heme pools in plastids and an altered heme turnover in the *PpTSPO1* mutants. Heme is an allosteric inhibitor of the glutamyl tRNA reductase that catalyses the second step of the 5-aminolevulinic acid (ALA) biosynthesis (Papenbrock and Grimm, 2001). If the elevated heme levels in the *PpTSPO1* knock-out lines can be ascribed to an increased plastidic heme concentration, the allosteric inhibition of the glutamyl tRNA reductase should result in reduced ALA synthesis rates. Indeed, measurement of ALA synthesis rates in wild-type plants and one *PpTSPO1* knock-out line in the presence of 250 mM NaCl revealed a reduced ALA synthesis rate in the *PpTSPO1* mutant line (Figure 6b). These data support enhanced plastidic heme accumulation as a consequence of PpTSPO1 deficiency. Furthermore, we applied ALA to liquid cultures of *P. patens* wild-type plants and one *PpTSPO1* knock-out line, which should result in a boost of the porphyrin synthesizing part of the tetrapyrrole biosynthesis pathway, because the synthesis of ALA is known to be the rate-limiting step in this pathway (Papenbrock and Grimm, 2001). Subsequently, the plant cultures were either grown in standard growth medium or in growth medium supplemented with 250 mM NaCl. To assess the role of PpTSPO1 for protoporphyrinogen allocation to mitochondria followed by heme synthesis, the accumulation of tetrapyrrole intermediates was determined after 6 and 12 h of ALA feeding under standard and salt-stress conditions. It is expected that upon a defective transport of protoporphyrinogen IX into the mitochondria, protoporphyrin IX will accumulate in the plastids and/or leak out into the cytoplasm (Jacobs *et al.*, 1990; Lee *et al.*, 1993; Li *et al.*, 2003). Between 6 and 12 h after ALA feeding of cultures in standard growth medium without NaCl, we measured increased but similar protoporphyrin IX concentrations in the wild type and the

PpTSPO1 knock-out line compared with the untreated control plants. Upon salt and ALA incubation, protoporphyrin IX levels increased even more in wild type and in the *PpTSPO1* knock-out line, but the protoporpyrin IX levels of the mutant line were two times higher compared with wild type (Figure 6c). This finding indicates an enhanced accumulation of the metabolic intermediate protoporphyrin IX in the mutant as a result of PpTSPO1 deficiency. It is assumed that this accumulated metabolite cannot be sufficiently directed to mitochondria, and remains non-metabolized in plastids and cytoplasm. To further prove this hypothesis, liquid cultures of the *PpTSPO1* knock-out lines and wild-type plants were treated with 30 μM acifluorfen in the presence of 350 mM NaCl. The diphenyl-ether herbicide acifluorfen inhibits plastidic as well as mitochondrial protoporphyrinogen IX oxidases, resulting in elevated levels of protoporphyrin IX (Becerril and Duke, 1989; Camadro *et al.*, 1991; Matringe and Scalla, 1988; Matringe *et al.*, 1989; Sherman *et al.*, 1991; Witkowski and Halling, 1988, 1989), which may accumulate in the plastids and/or leak into the cytosol. After 7 days of growth in the presence of acifluorfen and NaCl the *PpTSPO1* knock-out lines were completely bleached, whereas the wild-type plants remained green (Figure 6d). Furthermore, *PpTSPO1* knock-out lines grown in the presence of 350 mM NaCl without acifluorfen remained green, indicating that the bleaching was specifically caused by the inhibition of the protoporphyrinogen IX oxidases. From these data we conclude that PpTSPO1 is required to control protoporphyrin IX levels within the cytosol. Upon defective translocation of protoporphyrin IX into the mitochondria, protoporphyrin IX accumulates and elevated protoporphyrin IX concentrations induce photooxidative reactions including photobleaching within the plastids.

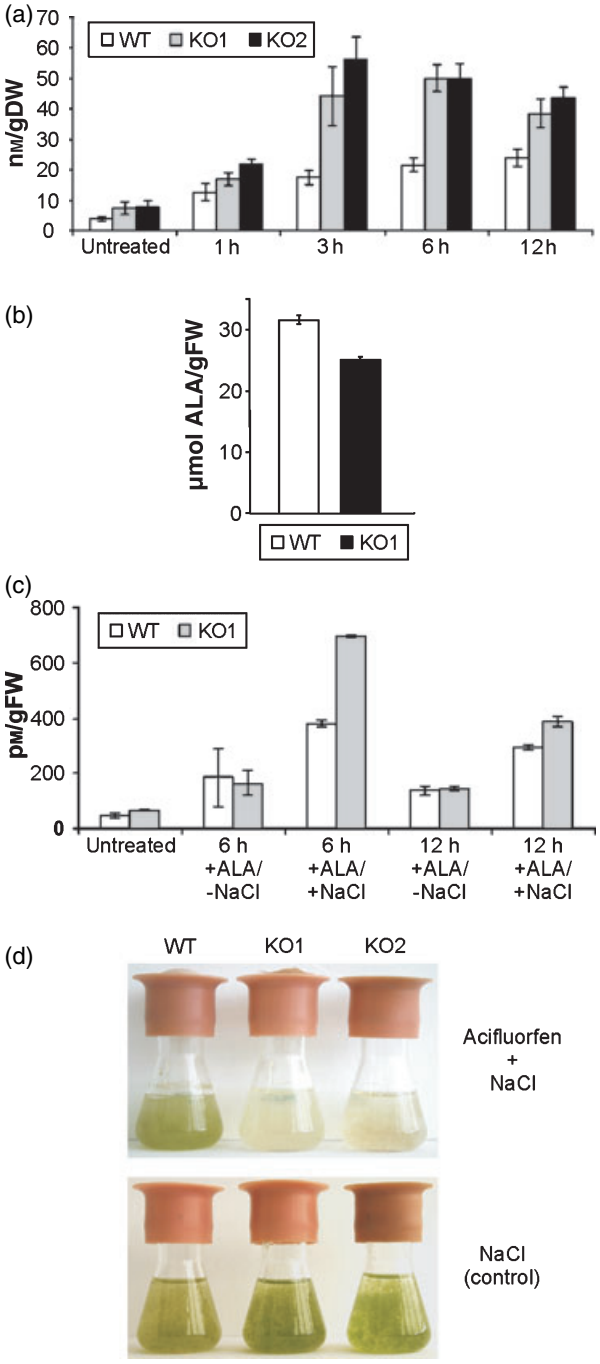

Figure 6. Measurements of heme and protoporphyrin IX concentrations, 5-aminolevulinic acid (ALA) synthesis rates and acifluorfen treatment in wild-type plants and *PpTSPO1* knock-out lines.
(a) Heme concentrations were determined after dehydration treatments at the indicated time points. Untreated plants served as controls. Error bars indicate SD (n = 3).
(b) ALA synthesis rates in wild-type plants (WT) and the *PpTSPO1* knock-out line 1 (KO 1).
(c) Protoporphyrin IX concentrations were determined at the indicated time points after feeding wild-type plants (WT) and the *PpTSPO1* knock-out line 1 (KO 1) with 500 μM ALA in standard growth medium (+ALA/–NaCl) and in growth medium supplemented with 250 mM NaCl (+ALA/+NaCl). Untreated plants (–ALA/–NaCl) served as controls. Error bars indicate SD (n = 3).
(d) Wild-type plants (WT) and *PpTSPO1* knock-out lines (KO 1, KO 2) were grown in the presence of 30 μM acifluorfen and 350 mM NaCl (Acifluorfen + NaCl). Cultures of wild-type plants and *PpTSPO1* knock-out lines grown in the presence of 350 mM NaCl (NaCl) served as controls. Pictures were taken 7 days after the start of the treatment.

Identification of PpTSPO1 *homologues*

The Arabidopsis genome contains only one TSPO-like protein (Lindemann *et al.*, 2004). An EST database search with the PpTSPO1 protein sequence as query revealed two additional homologues in *P. Patens*, which were designated *PpTSPO2* and *PpTSPO3*. Interestingly, compared with *PpTSPO1* the two identified genes encode shorter proteins of 175 and 180 amino acids, respectively, and lack the N-terminal region present in PpTSPO1. Moreover, PpTSPO2 and PpTSPO3 are more closely related to each other than to PpTSPO1 (Table 1; Figure S3). The mRNA levels of *PpTSPO2* and *PpTSPO3* were analysed by RNA gel blots with RNA

Table 1 Protein sequence comparison of PpTSPO1, PpTSPO2 and PpTSPO3 presented as a percentage of identity and similarity

	PpTSPO2	PpTSPO3
PpTSPO1	33% identity 44.5% similarity	33.5% identity 44.7% similarity
PpTSPO2		70.3% identity 78.9% similarity

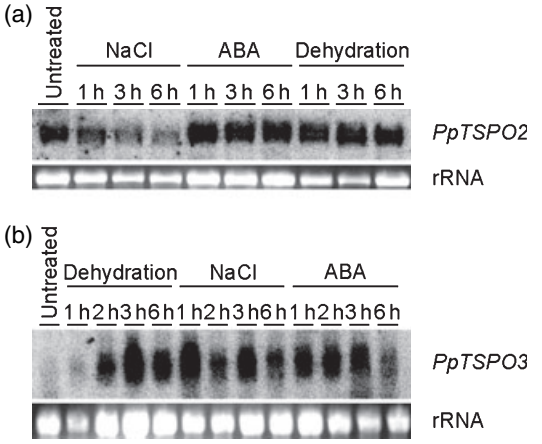

Figure 7. Expression analysis of *PpTSPO2* and *PpTSPO3*. *Physcomitrella patens* plants were dehydrated, treated with 20 μM abscisic acid or treated with 250 mM NaCl for the indicated time periods. Untreated control plants served as controls. A 10-μg sample of each RNA was loaded for RNA gel blots.
(a) RNA gel blot hybridized with the *PpTSPO2* probe.
(b) RNA gel blot hybridized with the *PpTSPO3* probe. The lower panel in each shows ethidium bromide stained rRNA bands to indicate equal loading of the samples.

from stressed and untreated *P. patens* wild-type plants (Figure 7a,b). *PpTSPO3* showed an abiotic stress and ABA-induced expression pattern similar to *PpTSPO1*. However, *PpTSPO2* was detected in all RNA samples, including RNA derived from untreated *P. patens* plants, indicating a constitutive expression.

Discussion

The existence of TSPO homologues in different kingdoms suggests a long-standing functional significance of this class of proteins during evolution. Consistent with the fact that mitochondria have originated from photosynthetic α-proteobacteria (Gray *et al.*, 2001), the eukaryotic TSPO homologues analysed so far were found to reside in mitochondria (Anholt *et al.*, 1986; Lindemann *et al.*, 2004), including the *P. patens* homologue PpTSPO1. Considering the common evolutionary background, the question arises if these proteins are also functionally related. In fact, TSPO homologues from plants, animals and bacteria bind benzodiazepine derivatives and PK11195, an isoquinilone carboxamide, with high affinity at nanomolar concentrations. In mammals, porphyrins are the predominant endogenous molecules with high affinity for the TSPO (Verma *et al.*, 1987). The TspO protein from *R. sphaeroides* is involved in the transport or efflux of tetrapyrrole intermediates of the heme and bacteriochlorophyll biosynthetic pathway (Yeliseev and Kaplan, 1999). Studies with the Arabidopsis TSPO-like protein indicated a functional role of this protein in the transport of protoporphyrin IX to mitochondria (Lindemann *et al.*, 2004).

The isolation of a stress-responsive homologue of the *TSPO* gene family from *P. patens* provides evidence for the involvement of this class of transporters in plant stress adaptation. The closest plant homologue of PpTSPO1 is encoded by a gene from the desiccation-tolerant moss *T. ruralis*. The corresponding mRNA was found to be among the most abundant transcripts identified from a *T. ruralis* cDNA library prepared from rapidly dried and subsequently rehydrated plants (Oliver *et al.*, 2004). Detailed expression data of TSPO homologues from seed plants have not yet been reported. Therefore, Arabidopsis gene expression data were analysed using the GENEVESTIGATOR microarray database (Zimmermann *et al.*, 2004). As for *PpTSPO1*, the microarray data reveal a stress-responsive expression pattern of the Arabidopsis homologue, with highest mRNA levels detected in response to salt and osmotic stress treatments. Most likely the transcriptional regulation depends on ABA, as indicated by increased mRNA levels upon treatment with ABA. However, mRNA levels in Arabidopsis do not considerably increase during dehydration and cold treatments, as observed for *PpTSPO1*. Elevated mRNA levels of the Arabidopsis *TSPO*-like gene were also detected during seed maturation, implying a role in desiccation processes and dormancy during seed maturation, as well as in stress adaptation.

The functional analysis of the *PpTSPO1* moss knock-out lines confirms an essential role of the encoded protein in abiotic stress adaptation. Based on its mitochondrial localization and presumable protoporphyrin transport activities, we hypothesize that PpTSPO1 plays a role in directing tetrapyrrole intermediates to mitochondria for heme production. We have indirect indications that PpTSPO1 is capable of transporting porphyrins, as we observed reduced chlorophyll autofluorescence in chloroplasts of cells transfected with the *PpTSPO1::GFP* overexpression construct. The reduced chlorophyll fluorescence observed in *PpTSPO::GFP*-overexpressing cells could be assigned to a possible disturbance of the porphyrin allocation between plastids and mitochondria.

It is proposed that an increased protoporphyrin import into mitochondria occurs in the adaptive response upon stress conditions for the delivery of substrates for heme bisosynthesis. Heme is the required co-factor for the ROS scavenging enzymes catalases and peroxidases. In animal cells, mitochondria are major sites of ROS formation, and major targets of ROS-induced damage (Kowaltowski and

Vercesi, 1999; Liu *et al.*, 2002). Also in plants, mitochondria have emerged to be a major source for ROS production caused by the interaction of oxygen with reduced forms of electron transport components (Moller, 2001). In particular, under stress conditions physical changes in membrane components may lead to constraints on the mitochondrial electron transport chain, resulting in enhanced ROS production (Wagner, 1995; Wagner and Krab, 1995). Studies on wheat indicated that mitochondria are the main target for oxidative damage. Even under normal growth conditions, mitochondria showed higher levels of oxidative damage compared with chloroplasts and peroxisomes. These levels were markedly increased upon drought conditions (Bartoli *et al.*, 2004). To overcome enhanced ROS production in mitochondria, plants possess specific alternative respiratory pathways that play a role in the control of ROS formation and scavenging. Among these, non-proton-pumping NAD(P)H dehydrogenases bypass complex I, and the alternative oxidase (AOX) accepts electrons directly from the ubiquinone pool without the intervention of the cytochrome *c* oxidase pathway through complexes III and IV (Rasmusson *et al.*, 1998). Nevertheless, once formed, ROS must be detoxified efficiently to minimize the consequential detrimental effects. Detoxifiying enzymes include superoxide dismutases (SODs) that convert the superoxide anion radical ($O_2^{-}\cdot$) to H_2O_2 and O_2 (Scandalios, 1993). MnSODs are found in mitochondria, and MnSOD expression often is upregulated by stress conditions (Bowler *et al.*, 1989; Tsang *et al.*, 1991). The main enzymatic H_2O_2 scavengers in plants are catalases and ascorbate peroxidases, which convert H_2O_2 to H_2O and O_2 (Asada, 1992; Willekens *et al.*, 1995). The mRNA levels of genes encoding catalases and ascorbate peroxidase increase upon different stress treatments (Dat *et al.*, 2000; Shigeoka *et al.*, 2002), and both enzymes need heme as a co-factor. Until now there was only limited knowledge about the role of catalases and ascorbate peroxidases in plant mitochondrial ROS scavenging. The existence of the ascorbate/glutathione cycle in plant mitochondria was shown in pea (Jimenez *et al.*, 1997), and, recently, the targeting of rice ascorbate peroxidase OSAPX6 to mitochondria was demonstrated (Teixeira *et al.*, 2006). Furthermore, the activity of several mitochondrial isoforms of ascorbate peroxidase increased upon salt treatment in the salt-tolerant tomato species *Lycopersicon pennellii* (Mittova *et al.*, 2004), suggesting a function in mitochondrial ROS scavenging. However, although the localization of catalase in mitochondria has been shown in animals (Radi *et al.*, 1991), its presence in plant mitochondria is still an open question. One plant catalase, CAT3 from maize, was found in mitochondrial fractions (Scandalios *et al.*, 1980), but further evidence for mitochondrial localization is missing. Interestingly, in potato both catalase and AOX are involved in the suppression of membrane potential breakdown, which triggers programmed cell death (Mizuno *et al.*, 2005). However, localization studies indicating mitochondrial targeting of the catalase have not been performed.

The measurement of heme contents in dehydrated *P. patens* wild-type plants indicated increasing heme levels during the dehydration process, which could reflect an enhanced demand for heme prosthetic groups upon abiotic stress conditions. However, during dehydration the two *PpTSPO1* mutant lines showed even higher heme levels compared with wild-type plants. These results could be interpreted as a stress-responsive induction of *PpTSPO1* that leads to enhanced heme biosynthesis in mitochondria. We believe that the elevated heme levels in the *PpTSPO1* knock-out lines result from increased plastidic heme synthesis in consequence of a block in mitochondrial uptake, and, accordingly, a redirection of plastid-remained protoporphyrin IX for the synthesis of plastid heme. This hypothesis was supported by the reduced ALA synthesis rate measured in the *PpTSPO1* knock-out line. In accordance with the effect of heme as an allosteric inhibitor of the glutamyl tRNA reductase, the elevated heme levels observed in the *PpTSPO1* mutants most likely can be ascribed to increased plastidic heme concentrations. Yet, an altered heme turnover in the *PpTSPO1* mutants can also not be excluded. However, in spite of the elevated heme levels, the *PpTSPO1* knock-out lines are more susceptible to abiotic stress conditions. Therefore, not the total quantity of heme, but rather its concentration in specific cellular compartments could be the critical factor for stress adaptation. In this case, the lack of heme groups in mitochondria could lead to reduced ROS scavenging and enhanced damage of mitochondrial components. In turn, mitochondrial dysfunction will result in elevated ROS levels affecting the redox homeostasis of the whole plant cell. The contribution of mitochondrial heme biosynthesis to the total intracellular heme pool is controversially discussed. In pea, the total mitochondrial heme biosynthetic activity was reported to be less than 10% compared with the activity detected in plastids, suggesting that plastids are the major site of heme biosynthesis (Cornah *et al.*, 2002). However, these studies did not include measurements of mitochondrial and plastidic heme biosynthesis under abiotic stress conditions. *In vivo* subcellular localization studies of the two cucumber ferrochelatases CsFeC1 and CsFeC2 revealed that both proteins are solely targeted to plastids (Masuda *et al.*, 2003). Based on this observation it must be considered that the mitochondrial heme biosynthetic pathway is lacking in particular plant species, and that the complete synthesis of heme is accomplished in the plastids. Nevertheless, the results obtained from our studies support the scenario of an enhanced demand for heme under stress conditions comprising the mitochondrial heme biosynthesis pathway.

Besides the allocation of porphyrin intermediates for mitochondrial heme biosynthesis, PpTSPO1 might also be involved in the removal of tetrapyrrole intermediates from

the cytosol. Tetrapyrrole intermediates are highly photoreactive, and, consequently, are a major source for the generation of ROS, especially under different abiotic stress conditions (Apel and Hirt, 2004; Mittler, 2002). The application of diphenylether herbicides, which inhibit protoporphyrinogen oxidase, led to the accumulation of protoporphyrin IX as a consequence of protoporphyrinogen IX oxidation in the cytoplasm (Jacobs *et al.*, 1990; Lee *et al.*, 1993; Li *et al.*, 2003). In turn, protoporphyrin reacts with light to produce singlet oxygen leading to lipid peroxidation, membrane disruption and cell death. In contrast, overexpression of a protoporphyrinogen oxidase gene in rice, and dual targeting of the enzyme into chloroplasts and mitochondria resulted in reduced oxidative stress after herbicide treatment (Jung and Back, 2005). Several experiments performed in this study support a function of PpTSPO1 in the distribution of tetrapyrrole intermediates in *P. patens*. Compared with wild-type plants, the *PpTSPO1* mutant lines were more susceptible to the herbicide acifluorfen, which causes increased protoporphyrin IX levels. Furthermore, the deleterious effect of NaCl in the *PpTSPO1* knock-out lines was more pronounced when the *PpTSPO1* knock-out lines were grown in light, which suggests a role of PpTSPO1 in the removal of photoreactive porphyrin intermediates. Finally, we detected elevated protoporphyrin IX levels in the *PpTSPO1* knock-out line in response to salt stress, which most likely is caused by the defective step of loading protoporphyrinogen into the mitochondria. Moreover, the resulting effects observed in the *PpTSPO1* knock-out lines are consistent with the studies mentioned above, where protoporphyrin IX accumulation was found to be a major cause for lipid peroxidation, membrane disruption and cell death. The efficient transport of porphyrins into mitochondria under abiotic stress conditions could result in reduced levels of photoreactive compounds, thereby limiting the generation of ROS.

Contrary to the situation in Arabidopsis, *P. patens* possesses two additional *TSPO* homologues. *PpTSPO2* and *PpTSPO3* encode shorter proteins, which lack the N-terminal region present in PpTSPO1, and could suggest a different subcellular targeting of both proteins. The use of bioinformatics protein localization prediction tools did not reveal unambiguous results for the localization of both proteins. To obtain a deeper insight into the function of this class of proteins, the subcellular targeting of both proteins must be analysed. However, the stress-responsive expression pattern of *PpTSPO3* suggests a role in the adaptation to adverse environmental conditions, as shown for *PpTSPO1*.

Experimental procedures

Plant material

Physcomitrella patens plants were cultured as previously described (Frank *et al.*, 2005a). Dehydration of plants, treatment with 250 mM NaCl and exogenous application of 20 μM ABA were performed as described by Frank *et al.* (2005b). Cold treatment of plants was performed by incubation of liquid cultures on ice. Treatments of liquid cultures with 0.5 μM methylviologen, 4 μM rotenone and 1 μM antimycin A, and 0.1% ethanol (control), were carried out at 25°C under constant light conditions of 110 μmol m^{-2} sec^{-1}. The ALA feeding was performed in standard growth medium supplemented with 500 μM ALA. For the salt treatment, NaCl was added at the appropriate time point at a concentration of 250 mM. For the acifluorfen treatment liquid cultures with 100 mg of plant material were grown in standard growth medium supplemented with 350 mM NaCl and 30 μM acifluorfen under normal growth conditions. Detection of the PpTSPO1::GFP fusion protein was performed 48 h after transformation of *P. patens* protoplasts, using 25 μg of the *PpTSPO1::GFP* fusion construct. Confocal laser scanning microscopy was carried out with an LSM510 Meta confocal microscope (Zeiss, http://www.zeiss.com) using 488-nm excitation and two-channel measurement of emission from 500–560 nm (green/GFP) as well as >590 nm (red/chlorophyll).

Measurement of ALA synthesis rates

Measurement of ALA synthesis upon treatment with levulinic acid (LA), a specific competitive inhibitor of ALA-dehydratase, was determined according to the method described by Goslings *et al.* (2004) with minor modifications. *P. patens* wild-type plants and a *PpTSPO1* knock-out line were grown in standard medium supplemented with 250 mM NaCl for 1 h in light, and then shifted to darkness with the addition of 80 mM LA for 6 h. Samples were harvested and immediately frozen in liquid nitrogen and stored at −80°C. Accumulated ALA was quantified as follows: samples were grinded and homogenized in 20% Trichloroacetic acid (TCA) (w/v), boiled for 15 min and centrifuged for 10 min (>14 000 ***g***). One volume of acetate buffer was added and the samples were centrifuged again for 10 min (>14 000 ***g***). After addition of 0.2 volumes of acetylacetone the samples were boiled for 10 min. After cooling on ice, one volume of freshly prepared modified Ehrlich's reagent was added. The samples were centrifuged for 5 min (>14 000 ***g***) and afterwards kept at room temperature (25°C) for 10 min. OD was determined at 553 nm. ALA concentrations were calculated according to an ALA calibration curve. The measurements were performed as three independent replications.

Molecular cloning

Differential display reverse transcription PCR (DDRT-PCR) was performed with total RNA derived from untreated, and 1-, 2-, 4- and 8-h dehydrated *P. patens* plants, respectively, using the GeneFishing DEG Kit 101 (Seegene, http://www.seegene.com). The *PpTSPO1* cDNA fragment was amplified with the provided arbitrary primer ACP4. A *PpTSPO1* full-length cDNA was identified from an internal EST database by BLASTN searches (Altschul *et al.*, 1997) and was sequenced. For the construction of a *PpTSPO1* knock-out construct, a *PpTSPO1* cDNA region was amplified using the following primers: 5′-GGATCCTTCAGAAGAGGAGCAGGGAC-3′ and 5′-GGATCCCAAATGTAAGGAAAGGATTGC-3′ (*Bam*HI restriction sites added to the primer sequences are underlined). A selection marker cassette (CaMV*35S* promoter::neomycin phosphotransferase::CaMV*35S* terminator) was amplified from the vector pRT101neo (Girke *et al.*, 1998) with the primers 5′-ACCGGTAACATGGTGGAGCACGACAC-3′ and 5′-ACCGGTACTGGATTTTGGTTTTAGGAA-3′ (*Age*I restriction sites added to the primers are underlined) and cloned into an *Age*I

restriction site present in the *PpTSPO1* cDNA. Before transformation, the *PpTSPO1* knock-out construct was released from the PCR4 TOPO vector by digestion with *Bam*HI. Primers used to identify *PpTSPO1* knock-out lines were: 5′-GTTCCACAGCGTCACTCTTG-3′ and 5′-CCAATAGCGATGGAATTCTCC-3′. The same primers have been used to confirm the loss of *PpTSPO1* transcript by RT-PCR. RT-PCR primers for the amplification of a *P. patens EF1α* homologue were: 5′-AGCGTGGTATCACAATTGAC-3′ and 5′-GATCGCTCGATCATGTTATC-3′. For the generation of a *PpTSPO1::GFP* fusion construct, the *PpTSPO1* open reading frame was amplified by PCR with the primers 5′-GGATCCATGAATTCCGAGGGTCTT-3′ and 5′-GGTACCATGACCACCACGACTATTC-3′ (*Bam*HI and *Kpn*I restriction sites added to the primers are underlined) and cloned into the *Bam*HI/*Kpn*I restriction sites of the GFP expression vector pMAV4 (Kircher *et al.*, 1999). The described *PpTSPO* knock-out lines are deposited in the International Moss Stock Center with the accessions IMSC-40110 and IMSC-40111.

Identification of homologues of PpTSPO1 *and glutathione peroxidases*

The following protein sequences were used to identify *P. patens* homologues by TBLASTN search of a *P. patens* EST database: PpTSPO1 protein sequence and the Arabidospsis glutathione peroxidase AAB52725.

RNA and DNA blot hybridization

Total RNA isolation and RNA blot hybridization were carried out as described by Frank *et al.* (2005b) using the following radioactively labelled cDNA probes: the dehydrin homologue *PpCOR47* (Frank *et al.*, 2005b); the *PpTSPO1* cDNA fragment, amplified by PCR using the primers 5′-GTTCCACAGCGTCACTCTTG-3′ and 5′-CCAATAGCGATGGAATTCTCC-3′; and cDNAs of *PpTSPO2*, *PpTSPO3* and the glutathione peroxidase homologue *PpGPX1* were all amplified with M13 primers present in the vector backbone. The cDNA fragment of the constitutively expressed gene *EF1α* was amplified using the primers described above. Genomic DNA was isolated as described by Bierfreund *et al.* (2003) and digested with the indicated restriction enzymes. Genomic blots of the *PpTSPO1* knock-out lines were hybridized with the complete *npt*II selection marker cassette.

H_2O_2 measurement

H_2O_2 was extracted as described by Rao *et al.* (2000). Briefly, 50 mg of plant material was ground to a powder under liquid nitrogen, and homogenized with 1 ml of 0.2 M $HClO_4$, held on ice for 6 min, centrifuged at 14 000 ***g*** for 15 min at 4°C and then neutralized to pH 7.0–8.0 with 0.2 M NH_4OH, pH 9.5. H_2O_2 was measured using the Amplex red H_2O_2/peroxidase assay kit (Invitrogen, http://www.invitrogen.com). The absorption of the oxidation product resorufin was measured spectrophotometrically at 570 nm, subtracting the value for non-specific absorbance at 595 nm. All experiments were performed as three independent replications.

Histochemical staining for H_2O_2

Production of H_2O_2 in wild-type plants and *PpTSPO1* knock-out lines was monitored by staining plants with 3, 3′-DAB, as previously described (Rea *et al.*, 2004), and then boiling in 96% ethanol for 10 min.

Cell-death measurement

Cell death was measured spectrophotometrically by Evans blue staining, indicating loss of plasma membrane integrity as described by Guo and Crawford (2005). Briefly, 50 mg of plant material was submerged in a 0.1% (w/v) aqueous solution of Evans blue (Sigma-Aldrich, http://www.sigmaaldrich.com) for 30 min followed by two 2-min cycles of vacuum. The plants were then washed three times with distilled water. Dye bound to dead cells was solubilized in 50% (v/v) methanol and 1% (w/v) sodium dodecyl sulphate at 60°C for 30 min and then quantified by measuring the absorbance at 600 nm. All experiments were performed as three independent replications.

Detection of lipid peroxidation

Lipid peroxidation in plants was analysed by measuring the level of malone dialdehyde, a decomposition product of the oxidation of polyunsaturated fatty acids, as described previously (Havaux *et al.*, 2003). Briefly, 50 mg of plant material was ground in 1 ml of chilled reagent [0.25% (w/v) thiobarbituric acid in 10% (w/v) trichloroacetic acid]. After incubation at 90°C for 20 min, the extracts were cooled at room temperature and centrifuged at 14 000 ***g*** for 20 min. The absorbance of the supernatant was measured at 532 nm, subtracting the value for non-specific absorbance at 600 nm. All experiments were performed as three independent replications.

Heme and protoporpyrin IX analysis

Heme was extracted from dried and frozen *P. patens* tissue as described by Weinstein and Beale (1984) with slight modification. The free heme and chlorophyll were removed from plant tissue with alkaline acetone. The non-covalently bound heme was extracted from the insoluble pellets with a mixture of one volume DMSO, five volumes of icy acetone and a quarter volume of concentrated HCl. The supernatants were transferred to ether, purified and concentrated on a CL-6B DEAE-Sepharose column (Amersham Biosciences, http://www.amersham.com). The level of heme was measured spectrophotometerically at 398 nm using the extinction coefficient 144 mM cm^{-1}. Protoporphyrin and Mg-protoporphyrins were extracted from frozen tissue with methanol, KH_2PO_4 buffer (pH 7.8) and PEX mixture [acetone, methanol, 0.1 N NH_4OH (10:9:1 v/v)]. Aliquots of the supernatant were separated by HPLC (Agilent, http://www.home.agilent.com) on an RP 18 column (Novapak C18, 4-μm particle size, 3.9 × 150 mm; Waters, http://www.waters.com) as described before (Alawady and Grimm, 2005). The porphyrins were identified and quantified by authentic standards purchased from Frontier Scientific (http://www.frontiersci.com). All measurements were performed as three independent replications.

Acknowledgements

We thank Edgar Wagner and Marco Vervliet-Scheebaum for their help performing the paraquat, rotenone and antimycin A inhibitor treatments. Financial support from the Deutsche Forschungsgemeinschaft in the scope of the Priority Program SPP1067 (Re837/7) and the Collaborative Research Centers (SFB) 388 is gratefully acknowledged. DR and EQ received fellowships from the German Academic Exchange Service (DAAD) and MW was supported by a fellowship from the Syrian Ministry of High Education.

Supplementary material

The following supplementary material is available for this article online:

Figure S1. Multiple protein sequence alignment of *PpTSPO1* homologues from bacteria, animals and plants.

Figure S2. Topology prediction of PpTSPO1 and its homologues.

Figure S3. Protein sequence alignment of PpTSPO1, PpTSPO2 and PpTSPO3.

Table S1. Homologues of the *Physcomitrella patens* PpTSPO protein from bacteria, plants and animals.

References

Alawady, A.E. and Grimm, B. (2005) Tobacco Mg protoporphyrin IX methyltransferase is involved in inverse activation of Mg porphyrin and protoheme synthesis. *Plant J.* **41**, 282–290.

Altschul, S.F., Madden, T.L., Schaffer, A.A., Zhang, J., Zhang, Z., Miller, W. and Lipman, D.J. (1997) Gapped BLAST and PSI-BLAST: a new generation of protein database search programs. *Nucleic Acids Res.* **25**, 3389–3402.

Anholt, R.R., Pedersen, P.L., De Souza, E.B. and Snyder, S.H. (1986) The peripheral-type benzodiazepine receptor. Localization to the mitochondrial outer membrane. *J. Biol. Chem.* **261**, 576–583.

Apel, K. and Hirt, H. (2004) Reactive oxygen species: metabolism, oxidative stress, and signal transduction. *Annu. Rev. Plant Biol.* **55**, 373–399.

Asada, K. (1992) Ascorbate peroxidase: a hydrogen peroxide scavenging enzyme in plants. *Physiol. Plant*, **85**, 497–504.

Bartoli, C.G., Gomez, F., Martinez, D.E. and Guiamet, J.J. (2004) Mitochondria are the main target for oxidative damage in leaves of wheat (*Triticum aestivum* L.). *J. Exp. Bot.* **55**, 1663–1669.

Beale, S.I. and Weinstein, J.D. (1990) Tetrapyrrole metabolism in photosynthetic organisms. In *Biosynthesis of Heme and Chlorophylls* (Dailey, H.A., ed). New York: McGeaw-Hill, pp. 287–391.

Becerril, J.M. and Duke, S.O. (1989) Protoporphyrin IX content correlates with activity of photobleaching herbicides. *Plant Physiol.* **90**, 1175–1181.

Bierfreund, N., Reski, R. and Decker, E.L. (2003) Use of an inducible receptor gene system for the analysis of auxin distribution in the moss Physcomitrella patens. *Plant Cell Rep.* **21**, 1143–1152.

Bowler, C., Alliotte, T., De Loose, M., Van Montagu, M. and Inze, D. (1989) The induction of manganese superoxide dismutase in response to stress in *Nicotiana plumbaginifolia*. *EMBO J.* **8**, 31–38.

Camadro, J.M., Matringe, M., Scalla, R. and Labbe, P. (1991) Kinetic studies on protoporphyrinogen oxidase inhibition by diphenyl ether herbicides. *Biochem. J.* **277 (Pt 1)**, 17–21.

Cornah, J.E., Roper, J.M., Pal Singh, D. and Smith, A.G. (2002) Measurement of ferrochelatase activity using a novel assay suggests that plastids are the major site of haem biosynthesis in both photosynthetic and non-photosynthetic cells of pea (*Pisum sativum* L.). *Biochem. J.* **362**, 423–432.

Cornah, J.E., Terry, M.J. and Smith, A.G. (2003) Green or red: what stops the traffic in the tetrapyrrole pathway? *Trends Plant Sci.* **8**, 224–230.

Dat, J., Vandenabeele, S., Vranova, E., Van Montagu, M., Inze, D. and Van Breusegem, F. (2000) Dual action of the active oxygen species during plant stress responses. *Cell Mol. Life Sci.* **57**, 779–795.

Dodge, A.D. (1971) The mode of action of the bipyridylium herbicides, paraquat and diquat. *Endeavour*, **30**, 130–135.

Frank, W., Decker, E.L. and Reski, R. (2005a) Molecular tools to study *Physcomitrella patens*. *Plant Biol. (Stuttg)* **7**, 220–227.

Frank, W., Ratnadewi, D. and Reski, R. (2005b) *Physcomitrella patens* is highly tolerant against drought, salt and osmotic stress. *Planta*, **220**, 384–394.

Girke, T., Schmidt, H., Zahringer, U., Reski, R. and Heinz, E. (1998) Identification of a novel delta 6-acyl-group desaturase by targeted gene disruption in *Physcomitrella patens*. *Plant J.* **15**, 39–48.

Goslings, D., Meskauskiene, R., Kim, C., Lee, K.P., Nater, M. and Apel, K. (2004) Concurrent interactions of heme and FLU with Glu tRNA reductase (HEMA1), the target of metabolic feedback inhibition of tetrapyrrole biosynthesis, in dark- and light-grown Arabidopsis plants. *Plant J.* **40**, 957–967.

Gray, M.W., Burger, G. and Lang, B.F. (2001) The origin and early evolution of mitochondria. *Genome Biol.* **2**, REVIEWS1018.

Grimm, B. (1998) Novel insights in the control of tetrapyrrole metabolism of higher plants. *Curr. Opin. Plant Biol.* **1**, 245–250.

Guo, F.Q. and Crawford, N.M. (2005) Arabidopsis nitric oxide synthase1 is targeted to mitochondria and protects against oxidative damage and dark-induced senescence. *Plant Cell*, **17**, 3436–3450.

Havaux, M., Lutz, C. and Grimm, B. (2003) Chloroplast membrane photostability in chlP transgenic tobacco plants deficient in tocopherols. *Plant Physiol.* **132**, 300–310.

Jacobs, J.M., Jacobs, N.J., Borotz, S.E. and Guerinot, M.L. (1990) Effects of the photobleaching herbicide, acifluorfen-methyl, on protoporphyrinogen oxidation in barley organelles, soybean root mitochondria, soybean root nodules, and bacteria. *Arch. Biochem. Biophys.* **280**, 369–375.

Jimenez, A., Hernandez, J.A., Del Rio, L.A. and Sevilla, F. (1997) Evidence for the presence of the ascorbate-glutathione cycle in mitochondria and peroxisomes of pea leaves. *Plant Physiol.* **114**, 275–284.

Jung, S. and Back, K. (2005) Herbicidal and antioxidant responses of transgenic rice overexpressing *Myxococcus xanthus* protoporphyrinogen oxidase. *Plant Physiol. Biochem.* **43**, 423–430.

Kircher, S., Wellmer, F., Nick, P., Rugner, A., Schafer, E. and Harter, K. (1999) Nuclear import of the parsley bZIP transcription factor CPRF2 is regulated by phytochrome photoreceptors. *J. Cell Biol.* **144**, 201–211.

Kircher, S., Gil, P., Kozma-Bognar, L., Fejes, E., Speth, V., Husselstein-Muller, T., Bauer, D., Adam, E., Schafer, E. and Nagy, F. (2002) Nucleocytoplasmic partitioning of the plant photoreceptors phytochrome A, B, C, D, and E is regulated differentially by light and exhibits a diurnal rhythm. *Plant Cell*, **14**, 1541–1555.

Kowaltowski, A.J. and Vercesi, A.E. (1999) Mitochondrial damage induced by conditions of oxidative stress. *Free Radic. Biol. Med.* **26**, 463–471.

Krishnamurthy, P.C., Du, G., Fukuda, Y., Sun, D., Sampath, J., Mercer, K.E., Wang, J., Sosa-Pineda, B., Murti, K.G. and Schuetz, J.D. (2006) Identification of a mammalian mitochondrial porphyrin transporter. *Nature*, **443**, 586–589.

Krogh, A., Larsson, B., von Heijne, G. and Sonnhammer, E.L. (2001) Predicting transmembrane protein topology with a hidden Markov model: application to complete genomes. *J. Mol. Biol.* **305**, 567–580.

Lee, H.J., Duke, M.V. and Duke, S.O. (1993) Cellular localization of protoporphyrinogen-oxidizing activities of etiolated barley (*Hordeum vulgare* L.) leaves (relationship to mechanism of action of protoporphyrinogen oxidase-inhibiting herbicides). *Plant Physiol.* **102**, 881–889.

Li, H. and Papadopoulos, V. (1998) Peripheral-type benzodiazepine receptor function in cholesterol transport. Identification of a putative cholesterol recognition/interaction amino acid sequence and consensus pattern. *Endocrinology*, **139**, 4991–4997.

Li, X., Volrath, S.L., Nicholl, D.B., Chilcott, C.E., Johnson, M.A., Ward, E.R. and Law, M.D. (2003) Development of protoporphyrinogen oxidase as an efficient selection marker for Agrobacterium tumefaciens-mediated transformation of maize. *Plant Physiol.* **133**, 736–747.

Lindemann, P., Koch, A., Degenhardt, B., Hause, G., Grimm, B. and Papadopoulos, V. (2004) A novel *Arabidopsis thaliana* protein is a functional peripheral-type benzodiazepine receptor. *Plant Cell Physiol.* **45**, 723–733.

Liu, Y., Fiskum, G. and Schubert, D. (2002) Generation of reactive oxygen species by the mitochondrial electron transport chain. *J. Neurochem.* **80**, 780–787.

Masuda, T., Suzuki, T., Shimada, H., Ohta, H. and Takamiya, K. (2003) Subcellular localization of two types of ferrochelatase in cucumber. *Planta*, **217**, 602–609.

Matringe, M. and Scalla, R. (1988) Studies on the mode of action of acifluorfen-methyl in nonchlorophyllous soybean cells: accumulation of tetrapyrroles. *Plant Physiol.* **86**, 619–622.

Matringe, M., Camadro, J.M., Labbe, P. and Scalla, R. (1989) Protoporphyrinogen oxidase as a molecular target for diphenyl ether herbicides. *Biochem. J.* **260**, 231–235.

McEnery, M.W., Snowman, A.M., Trifiletti, R.R. and Snyder, S.H. (1992) Isolation of the mitochondrial benzodiazepine receptor: association with the voltage-dependent anion channel and the adenine nucleotide carrier. *Proc. Natl. Acad. Sci. USA*, **89**, 3170–3174.

Mittler, R. (2002) Oxidative stress, antioxidants and stress tolerance. *Trends Plant Sci.* **7**, 405–410.

Mittova, V., Guy, M., Tal, M. and Volokita, M. (2004) Salinity upregulates the antioxidative system in root mitochondria and peroxisomes of the wild salt-tolerant tomato species *Lycopersicon pennellii*. *J. Exp. Bot.* **55**, 1105–1113.

Mizuno, M., Tada, Y., Uchii, K., Kawakami, S. and Mayama, S. (2005) Catalase and alternative oxidase cooperatively regulate programmed cell death induced by beta-glucan elicitor in potato suspension cultures. *Planta*, **220**, 849–853.

Moller, I.M. (2001) Plant mitochondria and oxidative stress: electron transport, NADPH turnover, and metabolism of reactive oxygen species. *Annu. Rev. Plant Physiol. Plant Mol. Biol.* **52**, 561–591.

Moulin, M. and Smith, A.G. (2005) Regulation of tetrapyrrole biosynthesis in higher plants. *Biochem. Soc. Trans.* **33**, 737–742.

Ohnishi, T., Sottocasa, G. and Ernster, L. (1966) Current approaches to the mechanism of energy-coupling in the respiratory chain. Studies with yeast mitochondria. *Bull. Soc. Chim. Biol. (Paris)* **48**, 1189–1203.

Oliver, M.J., Dowd, S.E., Zaragoza, J., Mauget, S.A. and Payton, P.R. (2004) The rehydration transcriptome of the desiccation-tolerant bryophyte *Tortula ruralis*: transcript classification and analysis. *BMC Genomics*, **5**, 89.

Papadopoulos, V. (1998) Structure and function of the peripheral-type benzodiazepine receptor in steroidogenic cells. *Proc. Soc. Exp. Biol. Med.* **217**, 130–142.

Papadopoulos, V., Boujrad, N., Ikonomovic, M.D., Ferrara, P. and Vidic, B. (1994) Topography of the Leydig cell mitochondrial peripheral-type benzodiazepine receptor. *Mol. Cell Endocrinol.* **104**, R5–R9.

Papadopoulos, V., Baraldi, M., Guilarte, T.R. *et al.* (2006) Translocator protein (18 kDa): new nomenclature for the peripheral-type benzodiazepine receptor based on its structure and molecular function. *Trends Pharmacol. Sci.* **27**, 402–409.

Papenbrock, J. and Grimm, B. (2001) Regulatory network of tetrapyrrole biosynthesis – studies of intracellular signalling involved in metabolic and developmental control of plastids. *Planta*, **213**, 667–681.

Persson, B. and Argos, P. (1994) Prediction of transmembrane segments in proteins utilising multiple sequence alignments. *J. Mol. Biol.* **237**, 182–192.

Persson, B. and Argos, P. (1996) Topology prediction of membrane proteins. *Protein Sci.* **5**, 363–371.

Radi, R., Turrens, J.F., Chang, L.Y., Bush, K.M., Crapo, J.D. and Freeman, B.A. (1991) Detection of catalase in rat heart mitochondria. *J. Biol. Chem.* **266**, 22028–22034.

Rao, M.V., Lee, H., Creelman, R.A., Mullet, J.E. and Davis, K.R. (2000) Jasmonic acid signaling modulates ozone-induced hypersensitive cell death. *Plant Cell*, **12**, 1633–1646.

Rasmusson, A.G., Heiser, V.V., Zabaleta, E., Brennicke, A. and Grohmann, L. (1998) Physiological, biochemical and molecular aspects of mitochondrial complex I in plants. *Biochim. Biophys. Acta*, **1364**, 101–111.

Rea, G., de Pinto, M.C., Tavazza, R., Biondi, S., Gobbi, V., Ferrante, P., De Gara, L., Federico, R., Angelini, R. and Tavladoraki, P. (2004) Ectopic expression of maize polyamine oxidase and pea copper amine oxidase in the cell wall of tobacco plants. *Plant Physiol.* **134**, 1414–1426.

Reinbothe, S. and Reinbothe, C. (1996) The regulation of enzymes involved in chlorophyll biosynthesis. *Eur. J. Biochem.* **237**, 323–343.

Richter, U., Kiessling, J., Hedtke, B., Decker, E., Reski, R., Borner, T. and Weihe, A. (2002) Two RpoT genes of *Physcomitrella patens* encode phage-type RNA polymerases with dual targeting to mitochondria and plastids. *Gene*, **290**, 95–105.

Scandalios, J.G. (1993) Oxygen stress and superoxide dismutases. *Plant Physiol.* **101**, 7–12.

Scandalios, J.G., Tong, W.F. and Roupaikas, D.G. (1980) Cat3, a third gene locus coding for a tissue-specific catalase in maize: genetics, intracellular location, and some biochemical properties. *Mol. Gen. Genet.* **179**, 33–41.

Schaefer, D.G. (2001) Gene targeting in *Physcomitrella patens*. *Curr. Opin. Plant Biol.* **4**, 143–150.

Sherman, T.D., Becerril, J.M., Matsumoto, H., Duke, M.V., Jacobs, J.M., Jacobs, N.J. and Duke, S.O. (1991) Physiological basis for differential sensitivities of plant species to protoporphyrinogen oxidase-inhibiting herbicides. *Plant Physiol.* **97**, 280–287.

Shigeoka, S., Ishikawa, T., Tamoi, M., Miyagawa, Y., Takeda, T., Yabuta, Y. and Yoshimura, K. (2002) Regulation and function of ascorbate peroxidase isoenzymes. *J. Exp. Bot.* **53**, 1305–1319.

Strepp, R., Scholz, S., Kruse, S., Speth, V. and Reski, R. (1998) Plant nuclear gene knockout reveals a role in plastid division for the homolog of the bacterial cell division protein FtsZ, an ancestral tubulin. *Proc. Natl. Acad. Sci. USA*, **95**, 4368–4373.

Taketani, S., Kohno, H., Okuda, M., Furukawa, T. and Tokunaga, R. (1994) Induction of peripheral-type benzodiazepine receptors during differentiation of mouse erythroleukemia cells. A possible involvement of these receptors in heme biosynthesis. *J. Biol. Chem.* **269**, 7527–7531.

Teixeira, F.K., Menezes-Benavente, L., Galvao, V.C., Margis, R. and Margis-Pinheiro, M. (2006) Rice ascorbate peroxidase gene family encodes functionally diverse isoforms localized in different subcellular compartments. *Planta*, **224**, 1–15.

Thompson, J.D., Higgins, D.G. and Gibson, T.J. (1994) CLUSTAL W: improving the sensitivity of progressive multiple sequence alignment through sequence weighting, position-specific gap penalties and weight matrix choice. *Nucleic Acids Res.* **22**, 4673–4680.

Tsang, E.W., Bowler, C., Herouart, D., Van Camp, W., Villarroel, R., Genetello, C., Van Montagu, M. and Inze, D. (1991) Differential

regulation of superoxide dismutases in plants exposed to environmental stress. *Plant Cell*, **3**, 783–792.

Verma, A., Nye, J.S. and Snyder, S.H. (1987) Porphyrins are endogenous ligands for the mitochondrial (peripheral-type) benzodiazepine receptor. *Proc. Natl. Acad. Sci. USA*, **84**, 2256–2260.

Wagner, A.M. (1995) A role for active oxygen species as second messengers in the induction of alternative oxidase gene expression in *Petunia hybrida* cells. *FEBS Lett.* **368**, 339–342.

Wagner, A.M. and Krab, K. (1995) The alternative respiratory pathway in plants. Role and regulation. *Physiol. Plant*, **95**, 318–325.

Weinstein, J.D. and Beale, S.I. (1984) Biosynthesis of protoheme and heme a precursors solely from glutamate in the unicellular red alga *Cyanidium caldarium*. *Plant Physiol.* **74**, 146–151.

Willekens, H., Inzé, D., Van Montagu, M. and Van Camp, W. (1995) Catalases in plants. *Mol. Breed*, **1**, 207–228.

Witkowski, D.A. and Halling, B.P. (1988) Accumulation of photodynamic tetrapyrroles induced by acifluorfen-methyl. *Plant Physiol.* **87**, 632–637.

Witkowski, D.A. and Halling, B.P. (1989) Inhibition of plant protoporphyrinogen oxidase by the herbicide acifluorfen-methyl. *Plant Physiol.* **90**, 1239–1242.

Yeliseev, A.A. and Kaplan, S. (1995) A sensory transducer homologous to the mammalian peripheral-type benzodiazepine receptor regulates photosynthetic membrane complex formation in *Rhodobacter sphaeroides* 2.4.1. *J. Biol. Chem.* **270**, 21167–21175.

Yeliseev, A.A. and Kaplan, S. (1999) A novel mechanism for the regulation of photosynthesis gene expression by the TspO outer membrane protein of *Rhodobacter sphaeroides* 2.4.1. *J. Biol. Chem.* **274**, 21234–21243.

Yeliseev, A.A., Krueger, K.E. and Kaplan, S. (1997) A mammalian mitochondrial drug receptor functions as a bacterial ''oxygen'' sensor. *Proc. Natl. Acad. Sci. USA*, **94**, 5101–5106.

Zimmermann, P., Hirsch-Hoffmann, M., Hennig, L. and Gruissem, W. (2004) GENEVESTIGATOR. Arabidopsis microarray database and analysis toolbox. *Plant Physiol.* **136**, 2621–2632.

Accession numbers for sequence data: Genbank accession numbers of the reported genes are *PpTSPO1* (DQ645822), *PpTSPO2* (DQ645820), *PpTSPO3* (DQ645823), *PpGPX* (DQ645821).

